Atom−Bond Pairwise Additive Representation for Cation−Benzene Potential Energy Surfaces: An ab Initio Validation Study

M. Albertí, A. Aguilar, and J. M. Lucas

CERQT, Departament de Química Física, Parc Científic, Universitat de Barcelona, Martí i Franquès, 1. 08028 Barcelona, Spain

F. Pirani

Dipartimento di Chimica, Università di Perugia, 06123 Perugia, Italy

D. Cappelletti

Dipartimento di Ingegneria Civile ed Ambientale, Università di Perugia, 06123 Perugia, Italy

C. Coletti and N. Re*

Dipartimento di Scienze del Farmaco, Università "G. d'Annunzio", Via dei Vestini 31, 66100 Chieti, Italy

Received: March 31, 2006; In Final Form: May 24, 2006

The achievement of extensive and meaningful molecular dynamics simulations requires both the detailed knowledge of the basic features of the intermolecular interaction and the representation of the involved potential energy surface in a simple, natural and analytical form. This double request stimulated us to extend to ion−molecule systems a semiempirical method previously introduced for the description of weakly interacting atom−molecule aggregates and formulated in terms of atomic species−molecular bond interaction additivity. The method is here applied to the investigation of the prototypical $M^+-C_6H_6$ systems (M = Li, Na, K, Rb and Cs) and some of its predictions are tested against accurate ab initio calculations. Such calculations have been performed by employing the MP2 method and large basis sets, privileging the description of the metal atoms. The agreement between potential energy scans semiempirically obtained and ab initio results is good for all the investigated geometries, thus showing that the adopted representation is in general able to reproduce all the main features of the potential energy surface for these systems. The role of the various noncovalent interaction components, as a function of the geometry and of the intermolecular distance in the $M^+-C_6H_6$ complexes, is also investigated for a more detailed assessment of the results of the semiempirical method.

1. Introduction

Intermolecular interactions affect a large number of matter properties.[1] In particular, noncovalent intermolecular interactions control several physical, chemical and biochemical processes, such as the energetics and geometry of weakly interacting aggregates,[2] competitive solvation of ions by different partners[3−5] and molecular recognition and selection.[6−8]

Noncovalent intermolecular interactions typically arise from the balancing of several components, like the electrostatic (of either attractive or repulsive nature), the exchange or size (of repulsive nature) and the induction and dispersion (of attractive nature). Unfortunately, it is quite difficult to accurately assess the relative role played by the various components of the interaction, some of them providing opposite contributions, to determine the main features of the full potential energy surface (PES). Therefore, it is often convenient, for investigating the dynamics at molecular level, to represent the global intermolecular reactions in terms of a few leading components. Moreover, a further challenging task is to provide a proper formulation of the dependence of such components on the intermolecular distance and on the geometry of the molecular aggregate, because most of its configurations are often very weakly bound and thus quite difficult to characterize. For these reasons, it is worth spending significant theoretical and experimental efforts to determine in detail the intermolecular interaction features, so to build their modeling on sound molecular science foundations.

Research activity on molecular aggregates involving aromatic and cyclic molecules has significantly grown in recent times,[6−38] because they are considered prototypical systems to investigate important processes, some of them indicated above.

In this paper we extensively investigate the alkali ion−benzene systems. A particularly noteworthy aspect of cation−π interaction is that their strength is several times greater than other interactions commonly involved in biological systems, such as hydrogen bonding and dispersion attractions, and this has recently attracted a great deal of interest due to the important role they may play in molecular recognition and in the structure and function of peptides and proteins.

The alkali ion−π interaction is characterized by a strong electrostatic component.[6−9,31,33] However, a description of the interaction solely in terms of a pure electrostatic component provides only a qualitative picture of the real situation.[31,32] In fact, as already mentioned, a complete and quantitative descrip-

* To whom correspondence should be addressed. E-mail: nre@unich.it.

10.1021/jp062007u CCC: $33.50
Published on Web 06/23/2006

tion of the noncovalent interaction can only be worked out by incorporating further ingredients such as the exchange, dispersion and induction components.[7−10] Unfortunately, in this respect, the available information concerns only the most stable configuration (see, for example, refs 9−11). In addition, experimental data are limited to formation enthalpies[6,7] and to dissociation energies[11] and, in the case of Na^+−benzene, the experimental results show some discrepancies.[11,39]

For all these reasons, we spent a significant amount of work to more quantitatively characterize the cation−π aromatic interactions, by considering the complete M^+−benzene aggregates series (M = Li, Na, K, Rb, Cs), to find the most appropriate formulation of the leading interaction components and to obtain the PESs in a simple analytical form, useful for molecular dynamics simulation.

A semiempirical method has recently been introduced[40] to describe atom−molecule systems and it is here extended to complexes involving closed shell ions and benzene (bz). Extensive ab initio calculations have also been performed to test the interaction potential energy at defined relative orientations of the M^+−bz complexes as a function of the intermolecular distance. Such a comparison is very useful to test the accuracy of the proposed semiempirical method and to define its potentialities and limitations. The paper is structured as follows: in section 2 we discuss the formulation of the PES, in section 3 the details of ab initio calculations are described, whereas results are presented and discussed in section 4. Concluding remarks are given in section 5.

2. Potential Energy Surface for M^+−Benzene Systems

A complete investigation of the static and dynamical properties of molecular aggregates requires an accurate description of the whole PES. This makes it important to adopt a functional representation of the intermolecular potential energy as a combination of a limited number of terms. These terms should represent the leading components of the interaction and, at the same time, they should be considered as "effective" components, because they include opposite contributions and effects due to the incomplete separability of the interaction energy. An important target of this study is thus to provide a functional representation of the PES that directly applies to the alkali ion series and that could be easily generalized to systems of increasing complexity.

Following the basic ideas of our semiempirical method,[40,41] the intermolecular interaction is formulated as arising from the combination of a (size) *repulsion* component and an (induction or dispersion) *attraction* component. The combination of such components is here defined as "nonelectrostatic" potential (V_{nel}), as opposite to the "electrostatic" one (V_{el}), describing the interaction between the ion and the quadrupole moment of benzene. Accordingly, the overall M^+−bz interaction, V_{total}, is formulated as

$$V_{total} = V_{nel} + V_{el} \tag{1}$$

where V_{nel} is given (see below) as a sum over twelve ion−bond terms, six of them describing the interactions between the ion and the C−C bonds and the remaining ones the interactions between the ion and the C−H bonds. V_{el} (see below) is described by means of a combination of Coulombic interactions between pairs of charges. The molecule is considered as a rigid body, but work is in progress to improve the description by including the dependence of the intermolecular interaction on internal coordinates. Results for K^+−bz have been already published and exploited in preliminary molecular dynamics simulations.[42]

In this paper the analysis focuses on the whole M^+−bz series. The validity of the method, together with an analysis of the different energy components, is tested by comparing its predictions with the outcome of ab initio calculations, as described in detail in the next section. A comparison with the available experimental information is also reported.

2.1. Nonelectrostatic Component. The nonelectrostatic component of the potential, V_{nel}, is given as a sum of twelve ion−bond interaction terms of the type[40]

$$V(r,\alpha) = \epsilon(\alpha)\left[\frac{m}{n(r,\alpha)-m}\left(\frac{r_m(\alpha)}{r}\right)^{n(r,\alpha)} - \frac{n(r,\alpha)}{n(r,\alpha)-m}\left(\frac{r_m(\alpha)}{r}\right)^{m}\right] \tag{2}$$

Such a simple formulation provides a realistic picture of both an effective *repulsion* (first term) and an effective *attraction* (second term). It also incorporates indirectly three body effects,[40] leads to a proper description of nonequilibrium geometries of the system[41] and can conveniently be used in molecular dynamics calculations. In eq 2, r is the distance of the ion from the bond center and α is the angle formed by $\vec{r}$ with the considered bond. To describe induction, which asymptotically represents the leading term of the attraction, the parameter m is set equal to 4 for all M^+−bond interactions. The parameter n, which defines the effective falloff of the ion−bond repulsion, is expressed as a function of both r and α using the equation

$$n(r,\alpha) = \beta + 4.0\left(\frac{r}{r_m(\alpha)}\right)^2 \tag{3}$$

where, at the beginning of the present investigation, β has been taken equal to 10 for all M^+−bond interactions.[40] However, some anomalies in the Li^+−bz system suggest that for such a system a smaller β value could be more appropriate (see section 4). The other important parameters ϵ and r_m, representing, respectively, the well depth and the equilibrium distance of the ion−bond pair, are assumed to depend on α according to the relationships

$$\epsilon(\alpha) = \epsilon_{\perp}\sin^2(\alpha) + \epsilon_{||}\cos^2(\alpha) \tag{4}$$

$$r_m(\alpha) = r_{m\perp}\sin^2(\alpha) + r_{m||}\cos^2(\alpha) \tag{5}$$

Reported values for parallel (||) and perpendicular ($\perp$) components of ϵ and r_m were derived using the charge and the polarizability of the involved atomic species as well as the polarizability and effective polarizability tensor components of aromatic C−C and C−H bonds, assumed to have an ellipsoidal shape whose center approximately coincides with that of the bond.[40,43] The whole procedure has been described in detail in ref 43 and applied for the first time to study the K^+−bz system.[42] This formulation of the potential also accounts for nonadditive effects via a controlled scaling of the polarizability values with respect to those shown by the isolated molecule (see, for example, ref 35). In particular, the employed polarizability values used for the calculations are 0.029 Å^3 for Li^+, 0.180 Å^3 for Na^+, 0.85 Å^3 for K^+, 1.410 Å^3 for Rb^+, 2.42 Å^3 for Cs^+,[44] 2.25 and 0.48 Å^3 for the parallel and perpendicular components of C−C bond, 0.79 and 0.58 Å^3 for the same components of C−H bond.[45] The values for C−H and C−C have been reduced by 15% and approximately 20%, respectively, to account for

TABLE 1: Cation−Bond Interaction Parameters

atom···bond	$\epsilon_\perp$/meV	$\epsilon_\parallel$/meV	$r_{m\perp}$/Å	$r_{m\parallel}$/Å
Li^+···C−C	50.83	147.46	2.509	2.826
Li^+···C−H	102.74	98.01	2.245	2.457
Na^+···C−C	33.01	102.20	2.848	3.149
Na^+···C−H	62.15	62.73	2.601	2.808
K^+···C−C[a]	22.95	75.77	3.266	3.547
K^+···C−H[a]	39.97	42.70	3.044	3.240
Rb^+···C−C	20.52	69.77	3.435	3.705
Rb^+···C−H	34.58	37.58	3.225	3.417
Cs^+···C−C	18.20	64.11	3.638	3.894
Cs^+···C−H	29.42	32.57	3.445	3.632

[a] Same values as in ref 42.

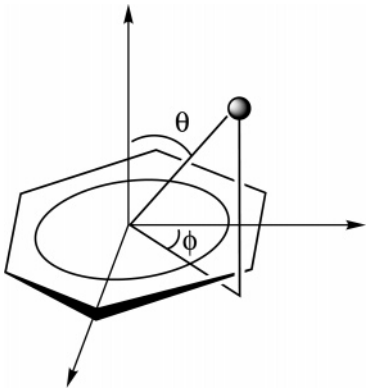

Figure 1. Polar coordinates R, θ, ϕ, defining the metal ion orientation with respect to the center of the benzene ring.

nonadditive effects in the ion−benzene interaction.[35,42] All the parameters for V_{nel} are given in Table 1. It must be remarked that these parameters are internally consistent, because they were obtained for all the systems by applying the same procedure, and that they are used to describe the intermolecular potential both for in-plane and for out-of-plane configurations.

2.2. Electrostatic Component. The electrostatic component V_{el}, which in the present case asymptotically corresponds to the ion−quadrupole interaction, is formulated, as suggested in refs 1 and 46 as a sum of Coulombic pair potentials. These potentials are associated with the interaction between the M^+ ion and both negative charges (placed on benzene C atoms on both sides of the aromatic ring) and positive charges (placed on benzene H atoms). The charges' sizes and their positions are chosen so as to reproduce the correct components of the benzene quadrupole moment.[47,48] This procedure leads to a charge of +0.09245 on each H atom and to two negative charges of −0.04623 (above and below the symmetry plane) separated by 1.905 Å on each carbon atom.

It is important to note that the present formulation of V_{total} involves the use of very few parameters, each one with a specific physical meaning. Furthermore, the usefulness of the adopted analytical form for V_{total} has been proved by recent molecular dynamics simulations.[42] Such formulation of the potential energy surface allows its analytical expression as a function of polar coordinates, R, representing the distance from the ion to the center of mass of the benzene molecule, and the polar angles θ and ϕ, defining the M^+ orientation with respect to benzene (see Figure 1).[41]

3. Ab Initio Calculations

High-level ab initio calculations have been performed to test the accuracy of the semiempirical PESs. Potential energy scans have been obtained by initially optimizing the geometry of benzene at the MP2/6-311+G* level of theory by assuming a D_{6h} symmetry. The center of mass of the optimized structure was then taken as the center of a polar coordinate system placing the metal cation at given radius R and polar angles θ and ϕ. Corrections to the basis set superposition error (BSSE), obtained following Boys−Bernardi counterpoise correction method,[49] have been included in all the calculations, which were carried out through the *Gaussian03* package.[50]

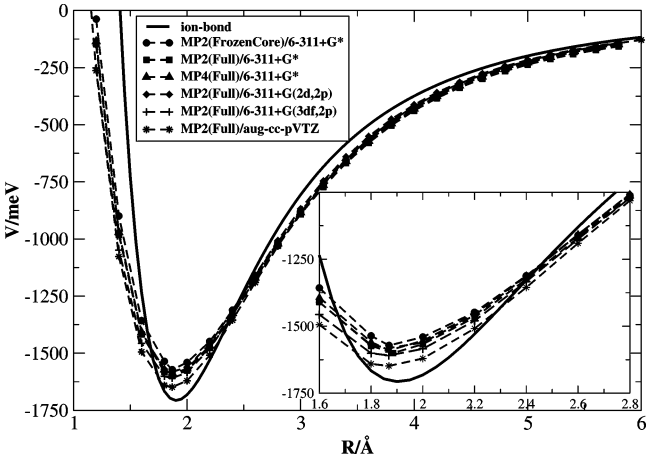

Figure 2. Potential energy curves for Li^+−benzene at $\theta = 0°$, as a function of R, calculated at different levels of theory and with the present semiempirical method.

For each system preliminary calculations have been carried out to evaluate the performance of different levels of theory in terms of accuracy and computational time. An example of such a comparison is depicted in Figure 2 for the Li^+−benzene complex along the C_{6v} symmetry axis as a function of R. The various levels of theory differ for the employed method and the basis set type, ranging from MP2(Frozen Core)/6-311+G*, MP2(Full)/6-311+G*, MP4(Full)/6-311+G*, MP2(Full)/6-311+G(2d,2p), MP2(Full)/6-311+G(3df,2p) to MP2(Full)/aug-cc-pVTZ, where here aug-cc-pVTZ indicates a mixed basis set, consisting of the augmented correlation-consistent triple-ζ basis set for the metal and carbon atoms and a 6-311+G* basis set for the hydrogen atom. As described in the following, the latter set was found to give the best performance and was employed for the description of Li^+ and Na^+ complexes and, with some modifications due to the unavailability of the aug-cc-pVTZ set for heavier metals, for the other alkali metal ion complexes.

Because a detailed discussion on the performance of the investigated methods and basis sets goes beyond the object of the present work, the interested reader is referred to ref 51. Here, as mentioned above, we report the results obtained with the level of theory which in each case gave the best agreement with the few available experimental data within a reasonable computational time. As emerged from recent ab initio studies on such systems,[11,36,37,54] a reliable description of alkali metal cation−benzene complexes requires both a high level electron correlation treatment and the use of large basis sets with the inclusion of, at least, $n - 1$ core electrons for the metal atom. In a recent paper[51] we have shown that the size of the basis set has a major impact on the accuracy of alkali metal ion−benzene binding energies, allowing for a significant improvement of the agreement between calculated and experimental bond dissociation energies[11] for heavier metal cations (Rb^+ and Cs^+).

For this reason all the calculations were performed with the second-order Møller−Plesset perturbation theory method (MP2) with large basis sets, emphasizing in particular the description of metal atoms. For Li^+− and Na^+−benzene complexes the aug-cc-pVTZ basis set described above has been used and all

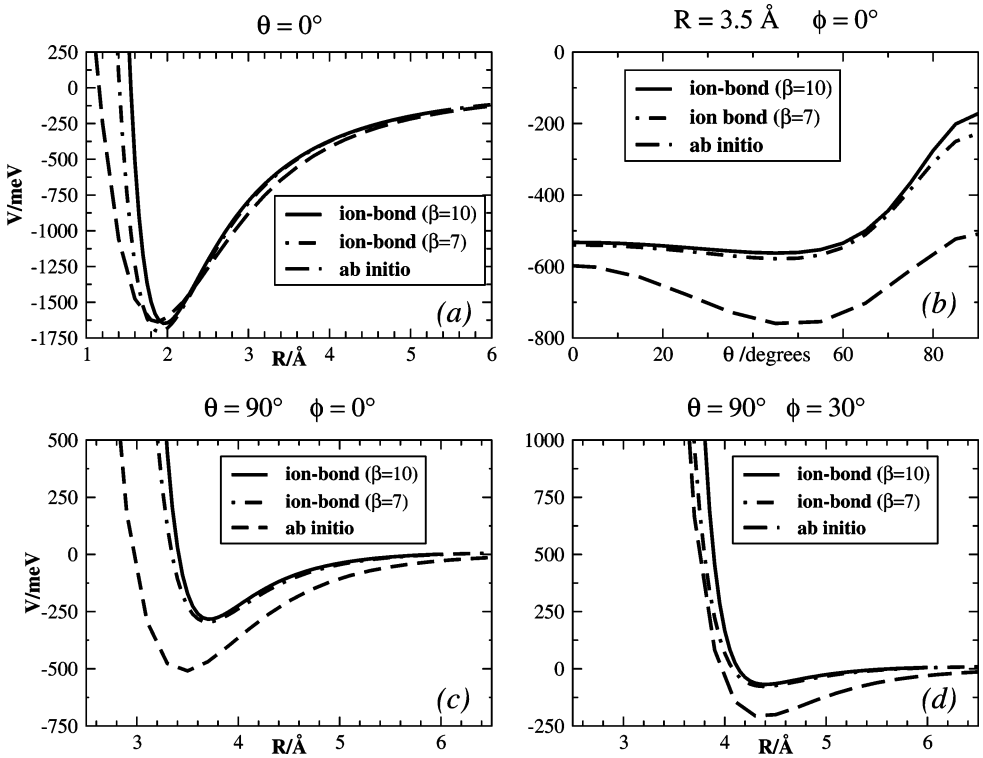

Figure 3. Potential energy curves at selected geometries for Li^+−benzene. β values refer to the use of eq 3.

core electrons (1s for C and Li, 1s, 2s and 2p for Na) have been included in the computations. Bond dissociation energies calculated with the present set, after correction for zero point vibrational energy (ZPE) contribution,[51] gave $D_0 = 1.54$ eV (experimental value from ref 11 1.67(0.14) eV) for Li^+−benzene and $D_0 = 0.94$ eV (experimental value from ref 11 0.96(0.06) eV and 0.99(0.06) eV from ref 56) for Na^+−benzene.

For potassium the aug-cc-pVTZ set was not available, we have thus used a 6-311+G(3df,2p) basis set for all atoms in K^+−benzene complex. Such a set was found[51] to often give results in good agreement with those obtained with the aug-cc-pVTZ set. The calculated bond dissociation energy D_0 in this case is 0.76 eV (experimental value $D_0 = 0.76(0.04)$ eV[11]).

Concerning the heavier metal cations (Rb^+ and Cs^+) we have used the Stuttgart relativistic, small core 1997 ECP basis set[55] consisting of a (7s6p)/[5s4p] contraction, to which we have added two polarization functions, d and f, so as to have a basis set comparable to those employed for the other heavy atoms. The exponents of the functions have been energy-optimized[51] and their values are 0.39 and 0.55 for Rb, and 0.29 and 0.44 for Cs. As in the calculations on Li^+− and Na^+−benzene complexes, we have used a aug-cc-pVTZ and a 6-311+G* basis set for the description of carbon and hydrogen, respectively. The bond dissociation energies obtained with this set,[51] $D_0 =$ 0.70 eV for Rb^+−benzene and $D_0 = 0.68$ eV for Cs^+−benzene, are in very good agreement with the corresponding experimental data,[11] 0.71(0.04) and 0.67(0.05) eV, respectively.

To compare the semiempirical values for electrostatic and nonelectrostatic contributions with ab initio results, an energy decomposition analysis according to Kitaura−Nakamura[53](KM) scheme has been carried out at the HF/6-311+G* level and reported for the Na^+−benzene complex. This level of theory, when BSSE corrections are not included, was found to give results in fairly good agreement with higher level ones. In any case, due to the qualitative nature of such a scheme, this comparison is not intended to be quantitative. Further analysis on the different contributions to the nonelectrostatic component of the energy, V_{nel}, have also been performed to investigate more in detail similarities and differences between the present model and ab initio results in the description of bonding in these systems. All energy decomposition calculations have been carried out using GAMESS−US software.[52]

4. Results and Discussion

Comparison between results of our semiempirical method and ab initio calculations are shown in Figures 3−7 for the whole M^+−bz family. The intermolecular potential is reported as a function of R or of the angle θ under four significant conditions: when the metal cation approaches along the benzene symmetry axis (panel *a*, $\theta = 0°$), at a fixed R value as a function of θ at $\phi = 0°$ (panel *b*) and in the benzene plane toward the center of the C−C bond (panel *c*, $\theta = 90°$ and $\phi = 0°$) or along the C−H bond direction (panel *d*, $\theta = 90°$ and $\phi = 30°$). The estimated uncertainties of the semiempirical results are ±0.08 eV for panel a and lower to ±0.04 eV for the other panels; uncertainties in the ab initio results are about ±0.04 eV.

In agreement with previous studies[7−11,56] the present investigation shows that all most stable equilibrium geometries are found when the M^+ ion is placed along the C_{6v} symmetry axis of the aromatic molecule. Moreover, as can be seen from Table 2, semiempirical and ab initio calculations give a dissociation energy, D_e, corresponding to the depth of the interaction potential well, which decreases with the mass of the M^+ ion, whereas the equilibrium distance, R_e, increases. Both semiempirical and ab initio values, when corrected for ZPE contributions, give results which are in good agreement, i.e., within respective uncertainties, with the bond dissociation energy, D_0, obtained by recent molecular beam experiments.[11,56]

The agreement between our semiempirical model and ab initio results is extremely good for heavier metal cations (K^+, Rb^+ and Cs^+), for which differences between the two approaches are minimal for all the considered geometries. Comparison of the equilibrium distances of the complexes in their more stable

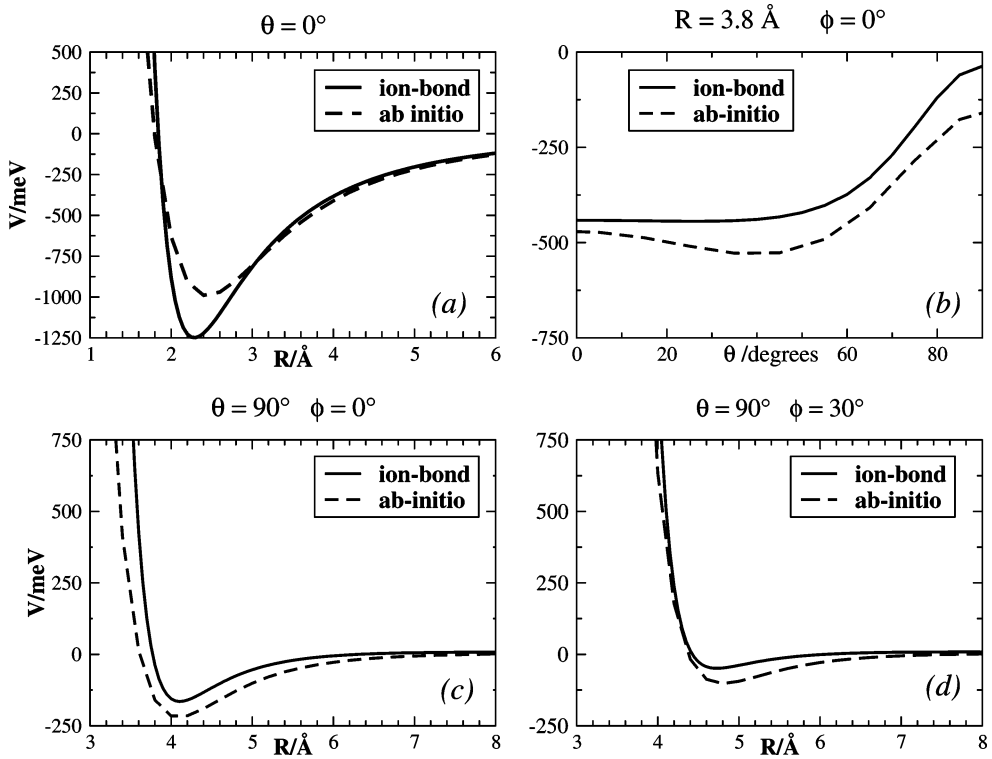

Figure 4. Potential energy curves at selected geometries for Na^+−benzene.

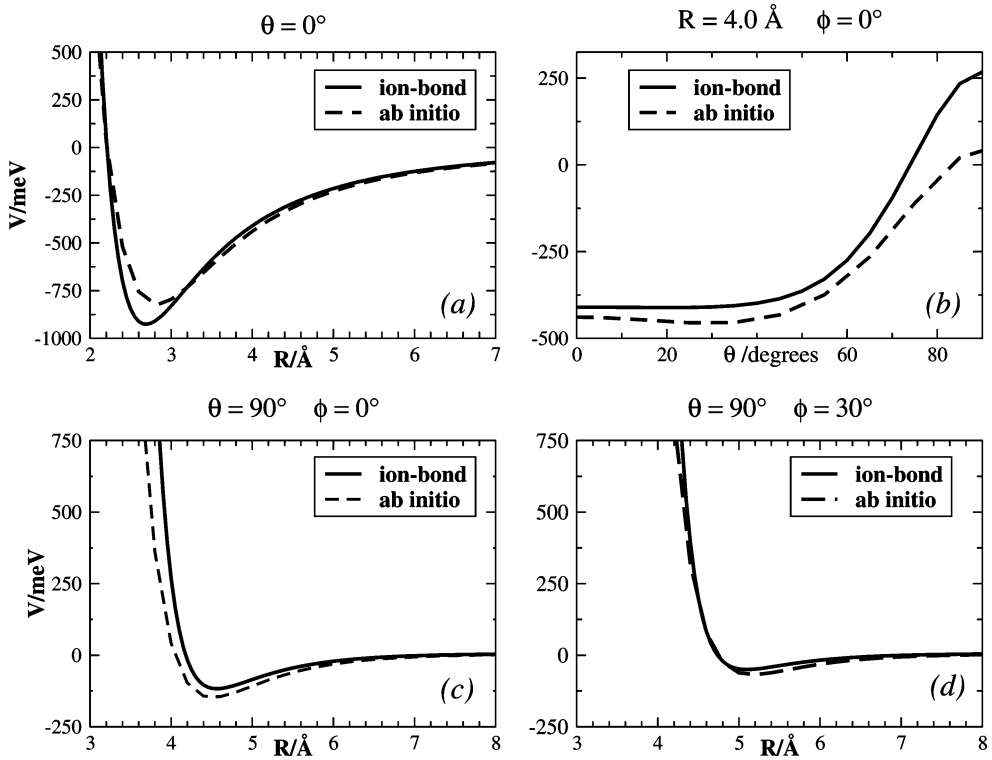

Figure 5. Potential energy curves at selected geometries for K^+−benzene.

configuration (Table 2) shows differences around 0.15 Å, with semiempirical values consistently smaller than the ab initio ones, with the only exception of Li^+−benzene, for which the semiempirical result is 0.1 Å larger. For the same configurations, bond dissociation energies are all within 0.1 eV (i.e., within the combined maximum uncertainties of the two methods), except for Na^+−benzene where a discrepancy of 0.25 eV is present (Table 2 and Figure 4a). However, for all the other considered geometries for this system (Figure 4, panels b−d) the semiempirical and ab initio curves lie very close.

For Li^+−benzene an analysis of the four panels of Figure 3 shows that ab initio calculations predict a less repulsive potential wall than the present model, which can also explain the correspondingly larger equilibrium distance (see above). Such an effect could be due to the penetration of the small Li^+ ion into the electron cloud of benzene, which cannot directly be

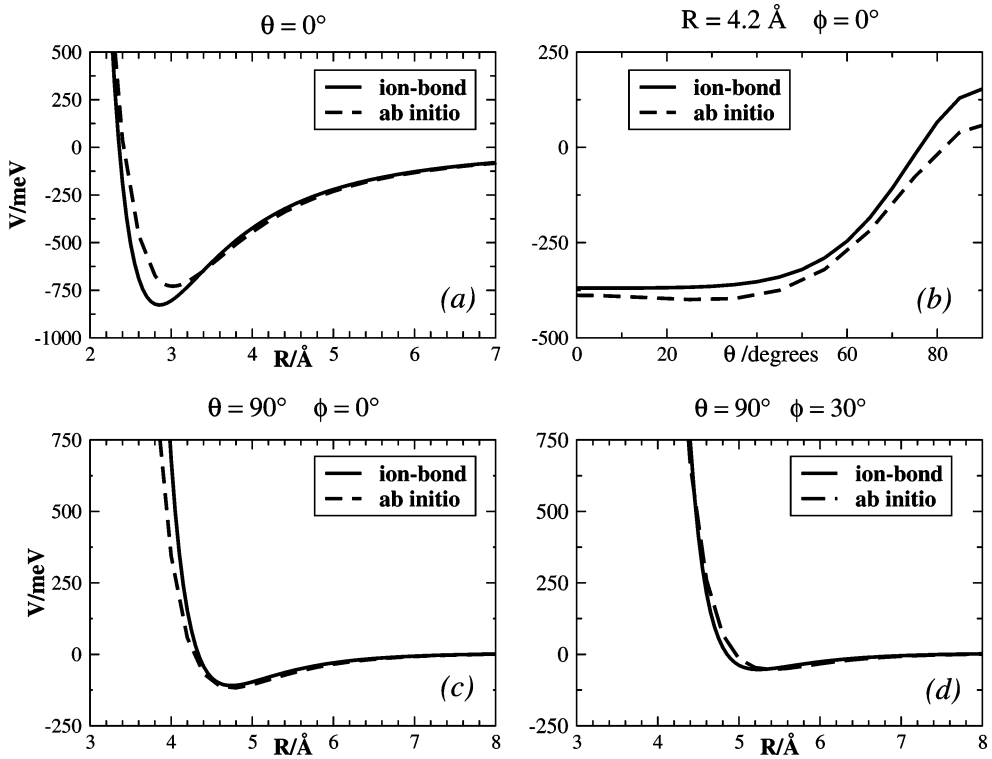

Figure 6. Potential energy curves at selected geometries for Rb^+−benzene.

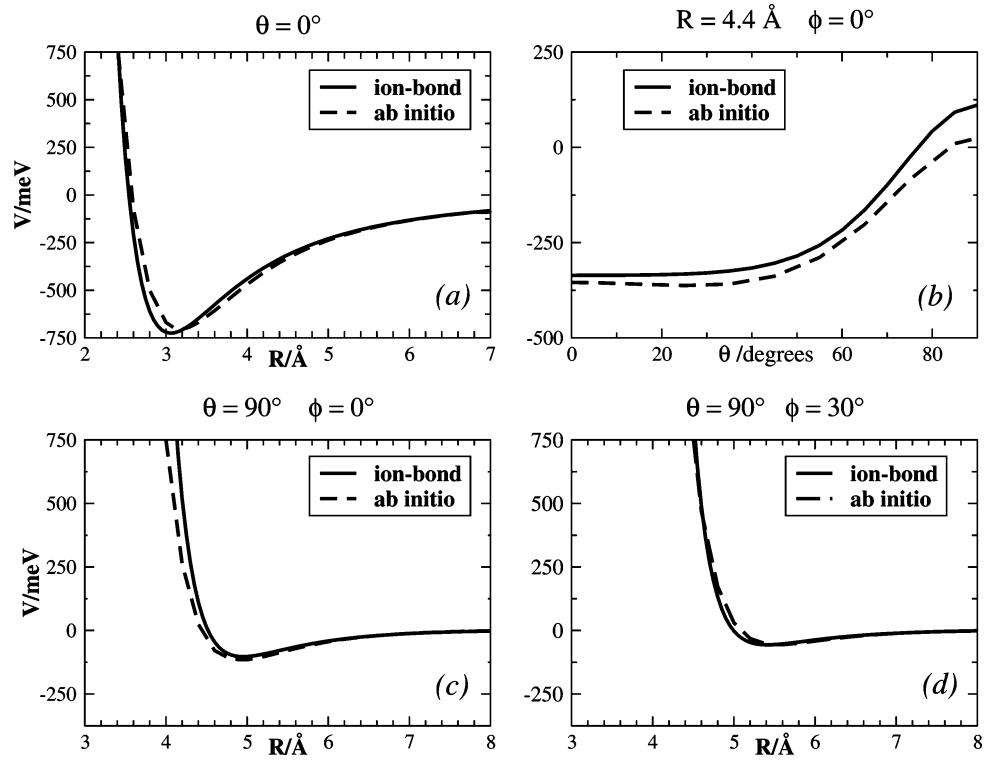

Figure 7. Potential energy curves at selected geometries for Cs^+−benzene.

considered in our semiempirical approach. It is possible, partially and only indirectly, to take this effect into account by reducing the value of the β parameter from 10 to 7 (Figure 3), as described in section 2. In any case the general topology of the PES is well reproduced also for this system.

A more detailed analysis of analogies and differences in the two approaches, which could also better explain the above-described anomaly in Li^+−bz system, can be carried out by comparing the single contributions to the total interaction energy. Indeed another advantage of the proposed semiempirical method lies in the fact that the electrostatic and nonelectrostatic components of V_{total} can be extracted in a straightforward way as a function of polar coordinates.

We have performed such analysis on Na^+−benzene, for the reasons outlined in the previous section, and Figure 8 reports V_{nel} and V_{el} values obtained semiempirically and calculated at HF/6-311+G* level of theory according to KM analysis. For all the reported configurations the qualitative behaviors of the

TABLE 2: Bold Dissociation Energy and Equilibrium Distances

system	D_e/eV (model)	D_e/Å (model)	D_e/eV (model)[f]	D_e/Å (ab initio)	D_0/eV (ab initio)	D_e/eV (model)	D_0/eV (exp)
Li^+-bz	1.648	1.97	1.558	1.63	1.87	1.54	1.67(0.14)[a] 1.57(0.08)[b]
Na^+-bz	1.249	2.29	1.196	0.990	2.44	0.937	0.99(0.06)[c] 0.96(0.06)[a] 1.2(0.06)[d]
K^+-bz	0.926	2.69	0.870	0.820	2.83	0.764	0.76(0.04)[a] 0.79(0.06)[e]
Rb^+-bz	0.828	2.86	0.801	0.728	3.02	0.701	0.71(0.04)[a]
Cs^+-bz	0.725	3.06	0.703	0.707	3.20	0.685	0.67(0.05)[a]

[a] Reference 11. [b] Reference 57. [c] Reference 56. [d] Reference 39. [e] Reference 46. [f] ZPE corrections for semiempirical results have been taken from the corresponding ab initio values, because they are expected to be close to (or, at most, a little larger than) the ab initio calculated ones.

semiempirical and ab initio curves are very similar, especially at large R distances. The electrostatic component, V_{el}, in particular, shows very small discrepancies both qualitatively and quantitatively at all R values. The only significant difference (but still rather small) is to be found in the position and depth of the well for the nonelectrostatic curve at $\theta = 0°$ (panel a).

It can be noticed that when the metal ion lies in the benzene plane ($\theta = 90$ °, panels c and d of Figure 8) the electrostatic curves have only been reported at $R > 3.3$ and $R > 3.8$ Å, respectively, for the two panels, because their representation at distances smaller than those corresponding to the repulsion wall between electronic shells has little meaning. In any case, the ab initio V_{el} component shows a decrease at small distances due to the increasing electrostatic attraction between the metal cation and the electron cloud of the C−C bond (panel c) and between the metal cation and the electron cloud of the hydrogen atom (panel d). In the simple point charge electrostatic representation of the present model the first of these effects comes into play at smaller distances, whereas the second one is absent.

The above-described difference in V_{nel} at $\theta = 0°$ (panel a, in Figure 8) can be assessed by further decomposing the nonelectrostatic contribution into its components. As described in section 2.1, in our semiempirical model V_{nel} is represented as a combination of an effective repulsion (whose leading contribution is ascribed to size effects) with an effective attraction (mainly determined by the induction). Both components of V_{nel} have been reported in Figure 9 for Na^+-benzene as a function of R at $\theta = 0°$. On the other hand, according to KM analysis, V_{nel} can be obtained as a sum of repulsive exchange and high order coupling terms (reported collectively in the figure for simplicity), of attractive polarization and charge transfer, here basically due to the penetration of the M^+ ion into the benzene electron cloud and depending on the ion−molecule orbital overlap, which exponentially decreases with R. To compare these interaction contributions, as provided by the two approaches (see Figure 9), one has to keep in mind that in the semiempirical method the attraction in V_{nel} is assumed to be nearly exclusively determined by induction effects, whereas all the remaining contributions are included in the repulsion component. We have therefore grouped the KM repulsion together with the charge transfer contribution, and the resulting interaction component is reported in Figure 9, so to be compared with the semiempirical repulsion. As shown in the figure, the KM induction contribution is larger than the corresponding semiempirical one, but this is counterbalanced by the larger repulsion. The presence of a charge transfer contribution, which is not explicitly included in the semiempirical approach, is probably responsible for most of the small discrepancies observed in the results for Na^+-benzene at short R (Figure 4). Indeed, as shown in Figure 9, charge transfer plays a significant role at $R < 4$ Å.

A similar analysis extended to the other metal cations reveals that charge transfer (i.e., the penetration effect) becomes less important as their mass increases. As a consequence, such a contribution can play some role for Li^+-benzene and, to a much

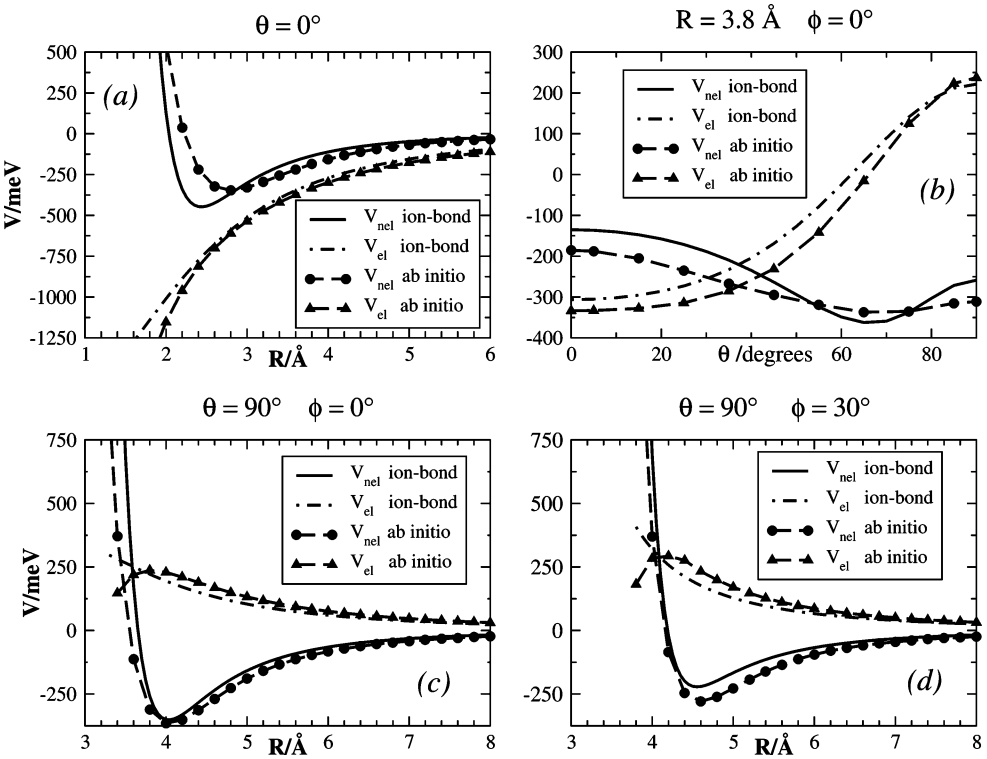

Figure 8. Electrostatic, V_{el}, and nonelectrostatic, V_{nel}, components of the potential energy for Na^+-benzene.

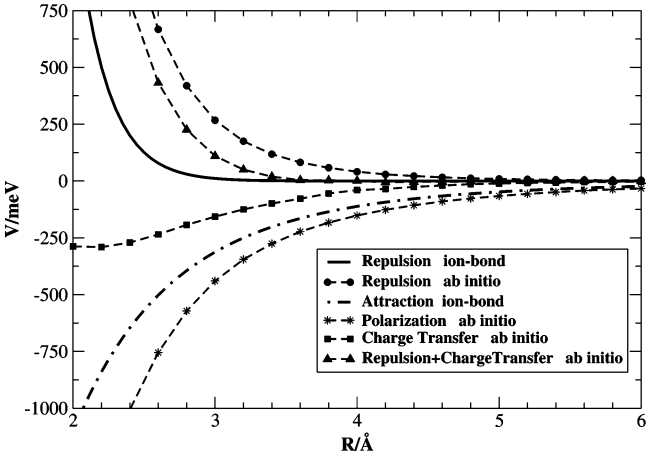

Figure 9. Energy contributions to V_{nel} for Na^+−benzene at $\theta = 0°$. The present semiempirical model consists of a repulsion (size) contribution and an attraction (polarization) contribution, whereas according to Kitaura−Morokuma[53] analysis the repulsion component is made of an exchange plus a higher order coupling, a polarization and charge transfer terms. Because in our semiempirical approach all the contributions other than induction are implicitly considered in the repulsion term, KM repulsion and charge-transfer terms have been grouped and their sum is also reported for comparison.

lesser extent, for Na^+−benzene, whereas it can be safely neglected for heavier metals. The penetration effect of the small Li^+ ion into the electronic cloud of the benzene molecule, expected to be maximum for $\theta = 0°$, can therefore partially account for the difference in the repulsive wall predicted by the two methods (panel a, Figure 3). This explains why a simple decrease of the β value in eq 3 leads to a better agreement between the two approaches. Indeed, a reduction of β determines a fall off of the global repulsion in V_{nel}.

Finally, the small or negligible role of chemical contributions in M^+−benzene systems can be justified by considering the benzene ionization potential, which appears to be significantly larger respect to that of M alkali metals. On the other hand, in the alkaline-earth dication−benzene systems, charge transfer is expected to play a more relevant role, leading to the opening of reactive channels at conical intersection between different potential energy surfaces.

5. Concluding Remarks

The present investigation focuses on the formulation of a semiempirical method, to predict and represent the intermolecular interaction in M^+−benzene systems, and on a critical analysis of its results, carried out by performing extensive ab initio calculations at defined geometries of the systems. Such a study shows that M^+−benzene systems mainly bind through noncovalent interactions.

The semiempirical method involves only few and effective interaction terms which are (i) representative of the leading interaction components, (ii) indirectly including the effect of other and less important interaction contributions, and (iii) expressed by simple functions but founded on solid physical grounds.

The role of the various components is compared with the results of extensive ab initio calculations, to test the validity of the adopted interaction decomposition procedure, and to define all the limitations of the global methodology. This is a basic information to devise possible extensions of this approach to more complex systems.

The possibility to represent the potential energy surface in a simple, natural and analytical form is crucial to carry out meaningful molecular dynamics simulation to clarify, for instance, the role of isomerization phenomena and the opening of dissociation channels when the total energy of the molecular aggregates is increased.

Acknowledgment. M.A., J.M.L. and A.A. acknowledge financial support from the Spanish DGICYT (Project CTQ2004-01102). Also thanks are due to the Centre de Supercomputació de Catalunya CESCA-C[4] for use of their computational facilities. D.C. and F.P. acknowledge financial support from the Italian Ministry of University and Research (MURST, PRIN 2004, Contract No. 2004033959_001 and PRIN 2005 Contract No. 2005033911_001). C.C. and N.R. acknowledge financial support from the Italian Ministry of University and Research (MURST, PRIN 2004, Contract No. 2004033959_003).

References and Notes

(1) Maitland, G. C.; Rigby, M.; Smith, E. B.; Wakeham, W. A. Intermolecular Forces, 2nd ed.;n., Oxford University Press: New York, 1987.
(2) Müller-Dethelfs, K.; Hobza, P. *Chem Rev.* **2000**, *100*, 143.
(3) Cabarcos, O. M.; Weinheimer, C. J.; Lisy, J. M. *J. Chem. Phys.* **1998**, *108*, 5151.
(4) Cabarcos, O. M.; Weinheimer, C. J.; Lisy, J. M. *J. Chem. Phys.* **1999**, *110*, 8429.
(5) Morais-Cabral, J. H.; Zhou, Y.; MacKinnon, R. *Nature* **2001**, *414*, 37.
(6) Kumpf, R. A.; Dougherty, D. A. *Science* **1993**, *261*, 1708.
(7) Dougherty, D. A. *Science* **1996**, *271*, 163.
(8) Ma, J. C.; Dougherty, D. A. *Chem. Rev.* **1997**, *97*, 1303.
(9) Tsuzuki, S.; Yoshida, M.; Uchimaru, T.; Mikami, M. *J. Phys Chem. A*, **2001**, *105*, 769.
(10) Kim, D.; Hu, S.; Tarakeshwar, P.; Kim, K. S.i; Lisy, J. M. *J. Phys. Chem. A* **2003**, *107*, 1228 and references therein.
(11) Amicangelo, J. C.; Armentrout, P. B. *J. Phys. Chem. A* **2000**, *104*, 11420.
(12) Ondrechen, M. J.; Berkovitch-Yellin, Z.; Jortner, J. *J. Am. Chem. Soc.* **1981**, *103* 6586.
(13) Fried, L. E.; Mukamel, S. *J. Chem. Phys.* **1991**, *96*, 116.
(14) Schmidt, M.; Le Calvè, J.; Mons, M. *J. Chem. Phys.* **1993**, *98*, 6102 and references therein.
(15) Cappelletti, D.; Bartolomei, M.; Aquilanti, V.; Pirani, F. *J. Phys. Chem. A*, **2002**, *106*, 10764.
(16) Pirani, F.; Porrini, M.; Cavalli, s.; Bartolomei, M.; Cappelletti, D.*Chem. Phys. Lett.* **2003**, *367*, 405.
(17) Mons, M.; Courty, A.; Schmidt, M.; Le Calvè, J.; Piuzzi, F.; Dimicoli, I. *J. Chem. Phys.* **1997**, *106*, 1676.
(18) Easter, D. C.; Bailey, L.; Mellot, J.; Tirres, M.; Weiss, T. *J. Chem. Phys.* **1998**, *108*, 6135.
(19) Schmidt, M.; Mons, M.; Le Calvè, J. *Chem. Phys. Lett.* **1991**, *177*, 371.
(20) Brupbacher, Th.; Makarewicz, J.; Bauder, A. *J. Chem. Phys.* **1994**, *101*, 9736.
(21) Hobza, P.; Bludsky, O.; Selzle, H. L.; Schalg, E. W. *Chem. Phys. Lett.* **1996**, *250*, 402.
(22) Lenzer, T.; Luther, K. *J. Chem. Phys.* **1996**, *105*, 10944.
(23) Bernshtein, V.; Oref, I. *J. Chem. Phys.* **2000**, *112*, 686.
(24) Dykstra, C. E.; Lisy, J. M. *J. Mol. Struct. (THEOCHEM)* **2000**, *500*, 375.
(25) Vacek, J.; Konvicka, K.; Hobza, P. *Chem. Phys. Lett.* **1994**, *220*, 85.
(26) Vacek, J.; Hobza, P. *J. Phys. Chem.* **1994**, *98*, 11034.
(27) Dullweber, A.; Hodges, M. P.; Wales, D. J. *J. Chem. Phys.* **1997**, *106*, 1530.
(28) Riganelli, A.; Memelli, M.; Laganà, A. *Lecture Notes in Comput. Science*, **2002**, *2331*, 926.
(29) Zoppi, A.; Becucci, M.; Pietraperzia, G.; Castellucci, E.; Riganelli, A.; Albertí, M.; Memelli M.; Laganà, A. Clustering properties of rare gas atoms on aromatic molecules, 16th International Symposium on Plasma Chemistry, Taormina, Italy June 22−27, 2003.
(30) Koch, H.; Fernández, B.; Makarewicz, J. *J. Chem. Phys.* **1999**, *111*, 198.
(31) Mecozzi, S.; West, A. P., Jr., Dougherty, D. A. *Proc. Natl. Acad. Sci. U.S.A.* **1996**, *93*, 10566.
(32) Mecozzi, S.; West, A. P.; Dougherty, D. A. *J. Am. Chem. Soc.* **1996**, *118*, 2307.
(33) Felder, C.; Jiang, H. L.; Zhu, W. L.; Chen, K. X.; Silman, I.; Botti, S. A.; Sussman, J. L. *J. Phys. Chem. A.* **2001**, *105*, 1326.

(34) Cubero, E.; Luque, F. J.; Orozco, M. *Proc. Natl. Acad. Sci. U.S.A.* **1998**, *95*, 5976.
(35) Caldwell, J. W.; Kollman, P. A. *J. Am. Chem. Soc.* **1995**, *117*, 4177.
(36) Nicholas, J. B.; Hay B. P.; Dixon, D. A. *J. Phys. Chem. A* **1999**, *103*, 1394.
(37) Feller, D.; Dixon, D. A.; Nicholas, J. B. *J. Phys. Chem. A* **2000**, *104*, 11414.
(38) Roncero, O.; Villarreal, P.; Delgado-Barrio, G.; Gonzlez-Platas, J.; Bretn, J. *J. Chem. Phys.* **1998**, *109*, 9288.
(39) Guo, B. C.; Purnell, J. W.; Castleman, A. W. *Chem. Phys. Lett.* **1990**, *168*, 155.
(40) Pirani, F.; Albertí, M.; Castro, A.; Moix, M.; Cappelletti, D. *Chem. Phys. Lett.* **2004**, *394*, 37.
(41) Albertí, M.; Castro, A.; Laganà, A.; Pirani, F.; Porrini, M.; Cappelletti, D. *Chem. Phys. Lett.* **2004**, *392*, 514.
(42) Albertí, M.; Castro, A.; Laganà, A.; Moix, M.; Pirani, F.; Cappelletti, D.; Liuti, G. *J. Phys. Chem. A* **2005**,*109*, 2906.
(43) Pirani, F.; Cappelletti, D.; Liuti, G. *Chem. Phys. Lett.* **2001**, *350*, 286.
(44) Cappelletti, D.; Liuti, G.; Pirani, F. *Chem. Phys. Lett.* **1991**, *183*, 297.
(45) (a) Denbigh, K. G. *Trans. Faraday Soc.* **1940**, *36*, 936. (b) Hirschfelder, J. O.; Curtiss, C. F.; Bird, R. B. Molecular Theory of Gases and Liquids, Wiley: New York, 1967.
(46) Sunner, J.; Nishizawa, K.; Kebarle, P. *J. Phys. Chem.* **1981**, *85*, 1814.
(47) Luhmer, M.; Bartik, K.; Dejaegere, A.; Bovy, P.; Reisse, J. *Bull. Soc. Chim. Fr.* **1994**, *131*, 603.
(48) Doerksen, R. J.; Thakkar, A. J. *J. Phys. Chem. A* **1999**, *103*, 10009.
(49) Boys, S. F.; Bernardi, R. *Mol. Phys.* **1970**, *19*, 553.
(50) *Gaussian03* Revision C.02, Frisch, M. J.; Trucks, G. W.; Schlegel, H. B.; Scuseria, G. E.; Robb, M. A.; Cheeseman, J. R.; Montgomery, J. A., Jr.; Vreven, T.; Kudin, K. N.; Burant, J. C.; Millam, J. M.; Iyengar, S. S.; Tomasi, J.; Barone, V.; Mennucci, B.; Cossi, M.; Scalmani, G.; Rega, N.; Petersson, G. A.; Nakatsuji, H.; Hada, M.; Ehara, M.; Toyota, K.; Fukuda, R.; Hasegawa, J.; Ishida, M.; Nakajima, T.; Honda, Y.; Kitao, O.; Nakai, H.; Klene, M.; Li, X.; Knox, J. E.; Hratchian, H. P.; Cross, J. B.; Bakken, V.; Adamo, C.; Jaramillo, J.; Gomperts, R.; Stratmann, R. E.; Yazyev, O.; Austin, A. J.; Cammi, R.; Pomelli, C.; Ochterski, J. W.; Ayala, P. Y.; Morokuma, K.; Voth, G. A.; Salvador, P.; Dannenberg, J. J.; Zakrzewski, V. G.; Dapprich, S.; Daniels, A. D.; Strain, M. C.; Farkas, O.; Malick, D. K.; Rabuck, A. D.; Raghavachari, K.; Foresman, J. B.; Ortiz, J. V.; Cui, Q.; Baboul, A. G.; Clifford, S.; Cioslowski, J.; Stefanov, B. B.; Liu, G.; Liashenko, A.; Piskorz, P.; Komaromi, I.; Martin, R. L.; Fox, D. J.; Keith, T.; Al-Laham, M. A.; Peng, C. Y.; Nanayakkara, A.; Challacombe, M.; Gill, P. M. W.; Johnson, B.; Chen, W.; Wong, M. W.; Gonzalez, C.; and Pople, J. A.; Gaussian, Inc., Wallingford CT, 2004.
(51) Coletti, C.; Re, N. *J. Phys. Chem. A* **2006**, *110*, 6563.
(52) Schmidt, M. W.; Baldridge, K. K.; Boatz, J. A.; Elbert, S. T.; Gordon, M. S.; Jensen, J. H.; Koseki, S.; Matsunaga, N.; Nguyen, K. A.; Su, S. J.; Windus, T. L.; Dupuis, M.; Montgomery, J. A. *J. Comput. Chem.* **1993**, *14*, 1347. URL: http://www.msg.ameslab.gov/GAMESS/GAMESS.html.
(53) (a) Kitaura, K.; Morokuma, K. *Int. J. Quantum Chem.* **1976**, *10*, 325. (b) Kitaura, K.; Morokuma, K. "Chemical Applications of Electrostatic Potentials", P.Politzer, D. G.Truhlar, Eds. Plenum Press: NY, **1981**, 215. (c) Chen, W.; Gordon, M. S. *J. Phys. Chem.* **1996**, *100*, 14316.
(54) Feller, D. *Chem. Phys. Lett.* **2000**, *322*, 543.
(55) Stuttgart Relativistic, Small Core basis set was obtained from EMSL Basis Set Library, at URL www.emsl.pnl.gov/forms/basisform.html. For the original valence basis set and ECP reference, see: Bergner, A.; Dolg, M.; Kuechle, W.; Stoll, H.; Preuss, H. *Mol. Phys.* **1993**, *80*, 1431.
(56) Amicangelo, J. C.; Armentrout, P. B. *Int. J. Mass Spectrom.* **2001**, *212*, 301.
(57) Woodin, R. L.; Beauchamp, J. L. *J. Am. Chem. Soc.* **1978**, *100*, 501.